AUTOMATIC DETECTION OF SMALL SPHERICAL LESIONS USING MULTISCALE APPROACH IN 3D MEDICAL IMAGES

Amir Fazlollahi[1, 2], Fabrice Meriaudeau[2], Victor L. Villemagne[3], Christopher C. Rowe[3], Patricia M. Desmond[4], Paul A. Yates[3], Olivier Salvado[1], Pierrick Bourgeat[1] and on behalf of the AIBL Research Group[5]

[1]The Australian e-Health Research Centre-BioMedIA, Royal Brisbane and Women's Hospital, Herston, QLD, Australia, 4029
[2]Le2i, Universite de Bourgone, Le Creusot, France, 71200

[3]Department of Nuclear Medicine and Centre for PET, Austin Hospital, Melbourne, VIC, Australia,
[4]Department of Radiology, Royal Melbourne Hospital, Melbourne University, VIC, Parkville, Australia;
[5]http://www.aibl.csiro.au/, Australia

ABSTRACT

Automated detection of small, low level shapes such as circular/spherical objects in images is a challenging computer vision problem. For many applications, especially microbleed detection in Alzheimer's disease, an automatic pre-screening scheme is required to identify potential seeds with high sensitivity and reasonable specificity. A new method is proposed to detect spherical objects in 3D medical images within the multi-scale Laplacian of Gaussian framework. The major contributions are (1) breaking down 3D sphere detection into 1D line profile detection along each coordinate dimension, (2) identifying center of structures by normalizing the line response profile and (3) employing eigenvalues of the Hessian matrix at optimum scale for the center points to determine spherical objects. The method is validated both on simulated data and susceptibility weighted MRI images with ground truth provided by a medical expert. Validation results demonstrate that the current approach has higher performance in terms of sensitivity and specificity and is effective in detecting adjacent microbleeds, with invariance to intensity, orientation, translation and object scale.

Index Terms— 3D sphere detection, Laplacian of Gaussian, cerebral micro bleed, center detection, multi-scale

1. INTRODUCTION

The task of identifying 3D sphere-like or 2D blob-like structures with variable size and intensity is of great importance: microaneurysms in fundus images [1], cerebral microbleeds in magnetic resonance imaging (MRI) [2] lung nodules in X-ray images [3]. For some application, an automatic pre-screening scheme is required to identify potential candidates as input for more elaborate decision algorithm. An ideal method must be reliable, scalable, and fast with a high level of sensitivity while allowing for some flexibility in the range of acceptable geometry of the detected lesions.

The majority of techniques are focused on vessel/line enhancement since sphere/blob detection is considered to be a sub-problem of line detection [4]. Template matching techniques are flexible and relatively straightforward to use for object localization. Yet it becomes less effective and slow for 3D images in the presence of shape and intensity variations. A majority of techniques use multiple isotropic Gaussian kernels to create a multi-scale representation while various response filters based on γ-normalized Laplacian of Gaussian (LoG) are developed for detection/enhancement of tubular-like and blob-like structures [4, 5, 6]. Furthermore, the filters adapt the eigenvalues of the Hessian to determine locally the likelihood that a primitive shape is present. The problem of false detection of outer corners has also been partially addressed [5, 7]. There has been, however few attempts to apply these methods to the detection of small lesions in 3D brain medical images. These lesions are generally modeled as solid spheres, with low and sometimes anisotropic spatial resolution, strong partial volume effects (PVE) making them appear relatively semi-spherical or ovoid in shape. Moreover, lesions adjacent to other structures with relatively higher contrast and larger size can remain undetected.

In this work a new technique for the identification of spherical structures of multiple sizes in 3D brain volume is proposed. The multiscale approach discussed here is inspired by the work of Lorenz *et al.* [8] who adapted multi-scale LoG and Hessian transform for vessel enhancement. Here, a lower false detection rate compared to state of the art methods is achieved by analyzing shape attributes associated with structures center point. The paper is organized as follows. Section 2 describes mathematical definition of multiscale LoG 1D line detection, shape center localization and sphericalness attribute. Experimental results evaluating the proposed method are explained in Section 3. Discussion

is presented in Section 4 and finally conclusions and future works are discussed in Section 5.

2. METHOD

The major contributions proposed here are summarized in 3 steps: (i) breaking down 3D sphere detection into multi-scale 1D line detection along x, y and z dimensions, (ii) identifying center of objects by combining normalized line response obtained in the previous step and finally (iii) employing eigenvalues of the Hessian matrix for the extracted center points in order to determine spherical objects.

2.1. Multi-scale 1D line detection

3D sphere detection can be considered a sub-problem of line detection in each dimension. Since shapes of interest can appear in different sizes, multi-scale space created by Gaussian smoothing at various extent is employed. The scale response filter, defined as the normalized second-order derivative of the smoothed image, has been widely used for describing curvatures [8, 9]:

$$R_{1D}(x;\sigma_{opt}) = \underset{\sigma}{ArgMin}\left(\sigma^{\gamma}\cdot\frac{d^2\,(I(x)*G(x;\sigma))}{dx^2}\right) \quad (1)$$

$$G(x;\sigma) = \frac{1}{\sigma\sqrt{2\pi}}e^{-x^2/2\sigma^2} \quad (2)$$

where R_{1D}, I, G and x are the response function at scale σ, gray-value image profile (with bright objects on top of a dark background), Gaussian kernel and pixel location, respectively. For I with dark objects on bright background, *Argmin* should be replaced by *ArgMax* in Eq. (1). The parameter γ in the term σ^{γ} was introduced to establish a normalized response at multiple scales since the Gaussian amplitude decreases as σ increases [9]. The scale σ_{opt} at which extremum response over all scales is attained, is assumed to give information about the size of the present structure. A line profile $I(x)$ in ideal case can be considered to be boxcar. However, due to PVE, lines usually do not appear with sharp edges and are closer to Gaussian profiles (Fig. 1.a) with maximum intensity c and width w given by:

$$I_G(x,\sigma=\frac{w}{2}) = c\cdot e^{\frac{-2x^2}{w^2}} = c\sqrt{\frac{\pi w^2}{2}}\cdot G(x;\frac{w}{2}) \quad (3)$$

$$I_B(x) = \begin{cases} c & if\ -w/2 \le x \le w/2 \\ 0 & otherwise \end{cases} \quad (4)$$

where I_G and I_B are Gaussian and boxcar line profile, respectively. The Parameter γ should be chosen so that an extremum over all scales can be achieved. Analytically, for the center of the line profiles at x=0, the desired extremum response is achieved when the size of the smoothing kernel matches the size of the profiles, meaning $\sigma_{opt}=\sigma=w/2$. This yields γ to be 1.5 for I_G and 2 for I_B in contrast with [8]. In order to fix γ for any arbitrary input, average value of 1.75 is chosen. The magnitude of the response profile R_{1D} is usually considered for localization: $R_{1D}<0$ is associated with bright lines while $R_{1D}>0$ is associated with dark lines and in both cases, there is a local extrema at the center of the structure (Fig. 1.b).

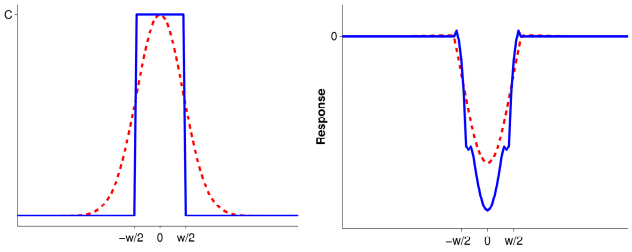

Fig. 1 (a) Boxcar and Gaussian line cross-section, (b) response function of Gaussian and boxcar line profile with γ=1.75

2.2. Centre detection

In most approaches, the center of the structure can be extracted as the maxima over the smoothed image profiles [7]. This is, however, not an effective method for multiple scales and adjacent structures.

In this work, a novel approach is proposed where the crossing of orthogonal line response profiles with an extremum in each dimension is regarded as a qualitative description of the structure center point. The response and its associated extremum are dependent on the shape extent, implying that intersect of each individual response may not necessarily be associated with the true center and can be biased. Here, this issue is addressed by normalizing the line response magnitude. The line center response which is expected to achieve the highest response magnitude can be considered as a reference point for normalization. By using equations (3) and (4) inside Eq. (1) for x=0, the line center response for I_G and I_B can be expressed as:

$$R_{1D-Gaussian}(0;\sigma_{opt}) = -0.38\times c\sigma_{opt}^{-3/4} \quad (5)$$

$$R_{1D-Boxcar}(0;\sigma_{opt}) = -0.48\times c\sigma_{opt}^{-1/4} \quad (6)$$

Likewise, this center response for any generic input can be estimated as summation of Eq. (5) and Eq. (6). Given that σ_{opt} is available from the previous step:

$$norm\ R_{1D}(x;\sigma_{opt}) = R_{1D}(x;\sigma_{opt})/((R_{1D-Gaussian}(0;\sigma_{opt}) + R_{1D-boxcar}(0;\sigma_{opt})) \quad (7)$$

where $normR_{1D}$ is the normalized response. The center map is then obtained by averaging the normalized line response of each dimension and extracting local maximas.

2.3. Sphere detection

In this step, a sphericalness measure is defined for the centers that are extracted in section 2.2 through Eigen

system of the Hessian matrix. The Hessian matrix encompasses the second order derivative which encodes local high-level shape information and the eigenvalues provide quantitative measure of the shape. The Hessian matrix is computed for each voxel in the image after the optimum scale is found through 3D LoG operator [10]. Several vesselness [4, 6, 11] and blobness filters [5] have been proposed using eigenvalues analysis of the Hessian.

For bright sphere on top of a dark background with corresponding eigenvalues of $|\lambda_1| \leq |\lambda_2| \leq |\lambda_3|$, a sphericalness attributes for each voxel x is defined as [12]:

$$S(x) = \begin{cases} 0 & \text{if } \lambda_1 > 0 \text{ or } \lambda_2 > 0 \text{ or } \lambda_3 > 0 \\ \dfrac{|\lambda_1|}{\sqrt{|\lambda_2 \lambda_3|}} & \text{otherwise} \end{cases} \quad (8)$$

The filter attains a maximum value of one at the center of a perfectly spherical object. In contrast with other studies where multiple criteria are combined to enhance and segment specific structures, here a single criterion is used for identification through a hard-thresholding scheme applied on the centers extracted in Section 2.2. S is invariant to grey-level re-scaling since it only involves the ratio of the eigenvalues. However, contrast variation across the shape due to noise or partial volume effects, can disturb the response value. To overcome this limitation, a threshold value of lower than expected anisotropy ratio should be considered.

3. RESULTS

The performance of the spherical object detection framework is assessed on different settings: the detection rate in clinical data and varying shape and intensity in simulated images. For better evaluation, the proposed method is compared to two other multi-scale techniques.

3.1. Simulated data

Existing blob/sphere filters show high response in outer corner of line-like structures such as vessels. Different criteria and parameters such as edge-indicator [8] and first derivatives [9] were proposed to address the problem of false detection. Though, presence of shape deformation, noise, contrast variation and presence of small scale structures can attenuate the performance.

In the initial step, to assess the performance of the proposed method, simulated synthetic data which is shown in Fig. 2.a is employed. The synthetic image volume includes tubular (26×3×3 and 26×5×5 pixels) and spherical (radius of 1.5, 2.5 and 4.5 pixels) shapes with varying intensity, orientation and located relatively close to each other. The proposed method is compared with two existing techniques: (A) multiscale vessel enhancement filter [6]

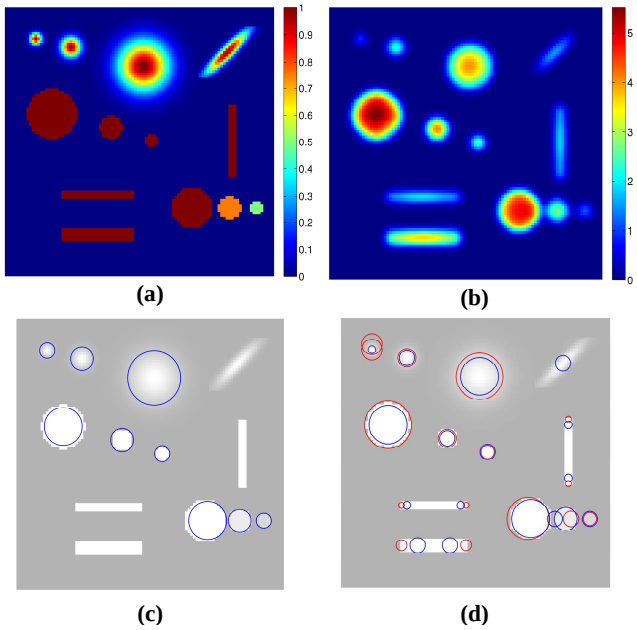

Fig. 2 (a) middle cross-section of the simulated image, (b) smoothed center detection response, (c) identified objects overlaid on the original image based on the proposed method, (d) identified objects based on method A (blue) and B (red).

which incorporates three geometric measures based on eigenvalues of Hessian. The associated parameters were empirically determined and adapted for spherical case, (B) multiscale blob detection technique proposed by [5] where the filter response has an additional term based on pre-determined size of objects along with eigenvalues ratio. Considering the objects size, multi-scale smoothing of [1:13] with step size of one is applied for all three techniques. The normalized center detection response is blurred by Gaussian with σ=1.5 to smooth out local peaks due to large multi-scale step size (Fig 2.b). Objects center were then identified by extracting the local maxima in this image. The multiscale sphere detection described in Section 2.3 was examined for each center point where value of 1 is expected for an ideal sphere. A low threshold value of 0.4 was used which allows detecting spherical/semi-spherical objects. The blobness filter in method B was adapted for 3D shapes by the same criterion as Eq. 8. The detection results of the proposed approach overlaid on the original image are shown in Fig. 2.c and Fig. 2.d.

Qualitative evaluation of the results showed that all the three methods are able to identify spherical objects, but methods A and B tend to generate multiple responses next to the edges. This is due to tubular structures appearing to be locally semi-spherical at the corners. This issue is addressed in the current method by restraining sphere response to the center of the object (described in Section 2.2). Method A, in contrast with the other methods, is less effective for identifying objects that are close to each other.

3.2. Clinical data

For further assessment of the current method, a subset of 30 subjects with Alzheimer's disease and mild cognitive impairment diagnosed with Cerebral Microbleeds (CMBs) from the Australian Imaging Biomarkers and Lifestyle (AIBL) study were included. CMBs are hypo-intense, nearly spherical structure on MRI and may vary in size (2-10mm) and contrast. For each subject, susceptibility weighted images (SWI) are available. 3D SWI was acquired on a 3-T Siemens TRIO scanner with 0.9×0.9 mm in-plane resolution and 1.75 mm slice thickness. SWI images were read by one expert. Finding CMBs in brain SWI image is a particularly challenging problem because of their small size, and their appearance on 2D slices which can be easily mistaken for vessel cross-sections or occlusions. SWI images were normalized to [0,1] after trimming the top 1% of intensity values within the brain mask. The images were also blurred by Gaussian with σ=0.5 to reduce the noise. For the multi-scale analysis, smoothing kernels of [1:5] with step size of 0.5 and sphericalness threshold of 0.4 were used Fig.3 shows the detected lesion overlaid on the pre-processed SWI image. To evaluate the performance of CMB detection, sensitivity and specificity rates of three available methods were computed and shown in Table 1. The proposed method shows 100% of sensitivity, where the other two methods left few CMBs undetected. Specificity is relatively high for all 3 methods which is due to large number of true-negatives. However, the proposed method yields on average 159 false detections per subject, while method A and B produce 710 and 421 false CMBs per subject, respectively.

Table 1. Evaluation of the method on real data

	Manual reads	Proposed method	Method A	Method B
True-positive	64	64	57	62
False-positive	-	4768	21301	12633
False-negative	-	0	7	2
True-negative	-	3599496	3582962	3591631
Sensitivity	100.0 %	100.0 %	89.0 %	96.9 %
Specificity	100.0 %	99.9 %	99.4 %	99.7 %

4. DISCUSSION

In this paper an automated technique for low-level identification of small lesions for 3D medical images was presented. The experimental results demonstrated that the method yields high level of sensitivity with relatively low false detection rate. This is achieved because it was designed to identify rather than enhancing/segmenting objects of interest which allows defining effective criteria to assess the presence of the object rather than assessing its extent.

Another advantage of the current method is that object center is accurately identified through combining normalized line filters. This also helps to detect the objects of interest adjacent to other structures. Since 1D line filter is considered to identify $\sigma_{opt,x}$,$\sigma_{opt,y}$ and $\sigma_{opt,z}$ independently, the object's local neighborhood would have different effects on the filter response of each dimension. Therefore, it is more likely to find the correct center for adjacent structures after the three responses are normalized and combined.

The present approach suffers from one limitation. The center detection step is not completely contrast and orientation invariant. Therefore it is possible that the detected center deviates from the true center or detect multiple centers if the contrast along the structure alters dramatically. However, Eigen system of the Hessian matrix which is employed in the final step can compensate as long as the detected center is close to the true center.

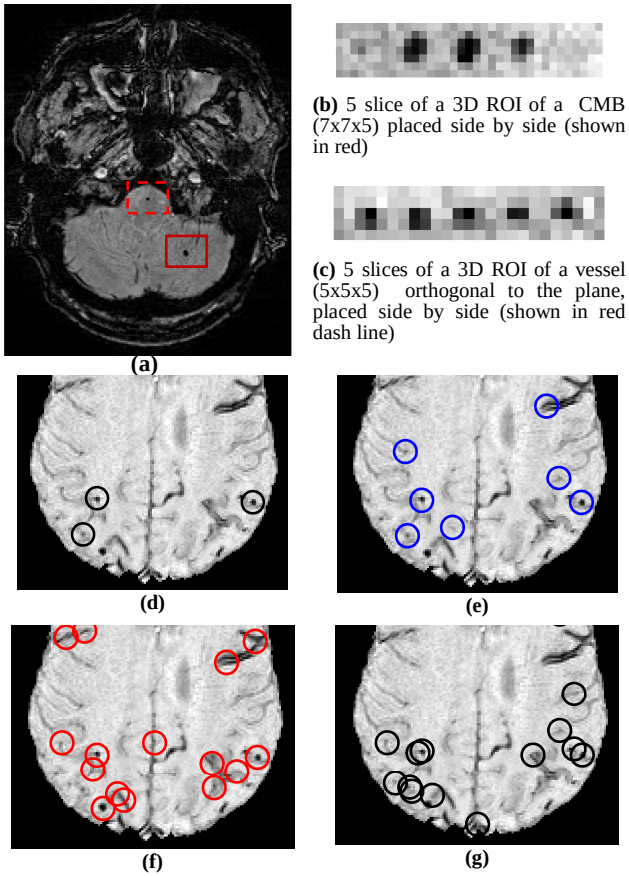

Fig. 3 (a) SWI cross-section and (d) examples of true CMBs (e) detection results of the current method (f) method A (g) and method B

5. CONCLUSION

A new multi-scale lesion detection method based on Laplacian of Gaussian was presented. It allows the detection of spherical/semi-spherical lesion in 3D brain images with high sensitivity and low false detection rate. Future work will look into combining this pre-selection step inside a complete classification system.

6. REFERENCES

[1] L. Giancardo, F. Meriaudeau, T.P. Karnowski, K.W. Tobin, Y. Li, and E. Chaum. Microaneurysms detection with the radon cliff operator in retinal fundus images. 7623:76230U–1, 2010.

[2] S.R.S. Barnes, E.M. Haacke, M. Ayaz, A.S. Boikov, W. Kirsch, and D. Kido. Semiautomated detection of cerebral microbleeds in magnetic resonance images. *Magnetic Resonance Imaging*, 2011.

[3] A. Schilham, B. van Ginneken, and M. Loog. Multi-scale nodule detection in chest radiographs. *Medical Image Computing and Computer-Assisted Intervention-MICCAI 2003*, pages 602–609, 2003.

[4] Y. Sato, S. Nakajima, H. Atsumi, T. Koller, G. Gerig, S. Yoshida, and R. Kikinis. 3d multi-scale line filter for segmentation and visualization of curvilinear structures in medical images. pages 213–222, 1997.

[5] J. Liu, J.M. White, and R.M. Summers. Automated detection of blob structures by hessian analysis and object scale. pages 841–844, 2010.

[6] A. Frangi, W. Niessen, K. Vincken, and M. Viergever. Multiscale vessel enhancement filtering. *Medical Image Computing and Computer-Assisted Interventation*, pages 130–137, 1998.

[7] S. Hinz. Fast and subpixel precise blob detection and attribution. *International Conference on Image processing*, 3:III–457, 2005.

[8] C. Lorenz, I. Carlsen, T. Buzug, C. Fassnacht, and J. Weese. Multi-scale line segmentation with automatic estimation of width, contrast and tangential direction in 2d and 3d medical images. pages 233–242, 1997.

[9] T.M. Koller, G. Gerig, G. Szekely, and D. Dettwiler. Multiscale detection of curvilinear structures in 2-d and 3-d image data. pages 864–869, 1995.

[10] T. Lindeberg. Feature detection with automatic scale selection. *International journal of computer vision*, 30(2):79–116, 1998.

[11] R. Manniesing, M.A. Viergever, and W.J. Niessen. Vessel enhancing diffusion: A scale space representation of vessel structures. *Medical Image Analysis*, 10(6):815–825, 2006.

[12] A.F. Frangi, W.J. Niessen, R.M. Hoogeveen, T. Van Walsum, and M.A. Viergever. Model-based quantitation of 3-d magnetic resonance angiographic images. *Medical Imaging, IEEE Transactions on*, 18(10):946–956, 1999.